

Electronic Structure of the High- T_c Superconductor $Ba_{1-x}K_xBiO_3$

L. F. Mattheiss and D. R. Hamann

AT&T Bell Laboratories, Murray Hill, New Jersey 07974

(Received 17 May 1988)

Band-structure results for ordered $Ba_{0.5}K_{0.5}BiO_3$ alloys confirm that the antibonding $Bi(6s)-O(2p)$ conduction band near E_F in cubic $BaBiO_3$ is minimally affected by substitutional K doping at the A (Ba) site. This supports the prediction that A -site doping would extend the metallic range of $Ba_{1-x}K_xBiO_3$ closer to half filling ($BaBiO_3$) than B -site doping ($BaPb_{1-y}Bi_yO_3$), thereby increasing both the coupling of the conduction electrons to bond-stretching O phonons and T_c . $Ba_{1-x}T_xPbO_3$, where T is trivalent, might also exhibit favorable superconducting properties.

PACS numbers: 74.70.Sw, 71.20.Cf, 71.25.Pi, 74.60.Mj

The discovery of high-temperature superconductivity ($T_c \approx 30$ K) in the La-Ba-Cu-O system by Bednorz and Müller¹ has stimulated an intensive search for new superconducting cuprate compounds with even higher T_c 's. There has been apparently less effort and certainly less success in the identification of new noncuprate superconductors with the potential for realization of transition temperatures in this range. One notable exception involves the Ba-K-Bi-O system. Recently, Mattheiss, Gyorgy, and Johnson² have reported evidence for superconductivity ($T_c \approx 22$ K) in minority fractions ($\approx 5\%$) of multiphase Ba-K-Bi-O samples with overall composition $Ba_{0.9}K_{0.2}BiO_3$. However, the chemical composition and structure of the superconducting phase were not identified. Cava *et al.*³ have since succeeded in synthesizing bulk single-phase Ba-K-Bi-O samples with superconducting onset temperatures as high as ≈ 30 K. More importantly, they have also determined the structure (cubic perovskite) and chemical composition ($Ba_{0.6}K_{0.4}BiO_{3-\delta}$) of the superconducting phase. The discovery of new noncuprate high- T_c materials should help elucidate the mechanism or mechanisms for the high superconducting transition temperatures.

The current focus on K- (or alkali-metal-) doped $Ba_{1-x}K_xBiO_3$ alloys was initiated by the 1975 discovery of Sleight, Gillson, and Bierstedt⁴ that $BaPb_{1-y}Bi_yO_3$ alloys exhibit superconductivity in the Pb-rich composition range $0.05 < y < 0.3$, with a maximum $T_c \approx 13$ K near $y \approx 0.25$. They found a metal-semiconductor transition near $y \approx 0.35$, with the semiconducting properties continuing to the end-member compound $BaBiO_3$. The benefit of doping at the perovskite A (or Ba) site rather than the B (or Pb-Bi) site to achieve higher T_c 's was suggested by the theoretical understanding that has evolved from extensive electronic-structure calculations for $BaPbO_3$, $BaBiO_3$, and the intermediate $BaPb_{1-y}Bi_yO_3$ alloys.⁵⁻⁹

According to these studies, the undistorted cubic $BaPb_{1-y}Bi_yO_3$ alloys possess a single broad conduction band that involves σ -antibonding combinations of Pb- $Bi(6s)$ and $O(2p)$ states. This band is gradually filled in

rigid-band fashion with increasing y until it is half filled in $BaBiO_3$. Here, a combination of Fermi-surface nesting and the strong coupling of the conduction-band states near E_F to bond-stretching O displacements leads to a commensurate charge-density-wave distortion in which the O octahedra surrounding adjacent Bi sites are alternately expanded or compressed.¹⁰ As the calculations show,⁷ this breathing displacement of neighboring O octahedra opens a semiconductor gap at E_F , thereby explaining the semiconducting properties of $BaBiO_3$.

The mechanism by which the semiconducting properties of $BaPb_{1-y}Bi_yO_3$ are extended over intermediate compositions $0.35 < y < 1$ is less well understood. A proposal by Weber¹¹ attributes this semiconducting behavior to a combination of static incommensurate "breathing-type" charge-density waves and chemical "ordering waves" on the Pb-Bi sublattice. Indeed, large (≈ 1 eV) superlattice splittings are found^{9,12} for Pb-Bi ordering at the active B site in $BaPb_{0.5}Bi_{0.5}O_3$ alloys. However, since the wave-function amplitude for conduction-band states is small at the Ba sites,⁵⁻⁹ A -site substitution should have a reduced effect. Accordingly, Mattheiss, Gyorgy, and Johnson² proposed to leave the conducting Bi-O complex intact and to vary the filling of the antibonding $Bi(6s)-O(2p)$ conduction band by substitutional alkali-metal doping at the inactive Ba donor sites. As the findings of Cava *et al.*³ confirm, this extends the metallic range in $Ba_{1-x}K_xBiO_3$ closer to half filling ($BaBiO_3$) where the electron-phonon interaction is a maximum,^{7,13} thereby producing materials of marginal stability with enhanced T_c 's.

The objective of the present investigation is to determine the extent to which substitutional K doping at the Ba site alters the electronic band properties near E_F for the $Ba_{1-x}K_xBiO_3$ alloys in the composition range ($x \approx 0.4$) where the highest T_c 's have been observed thus far. As a means for addressing this issue, self-consistent linear augmented-plane-wave (LAPW) calculations have been carried out for three different 50-50 $Ba_{0.5}K_{0.5}BiO_3$ ordered alloys. The present implementation¹⁴ of the LAPW method imposes no shape approxi-

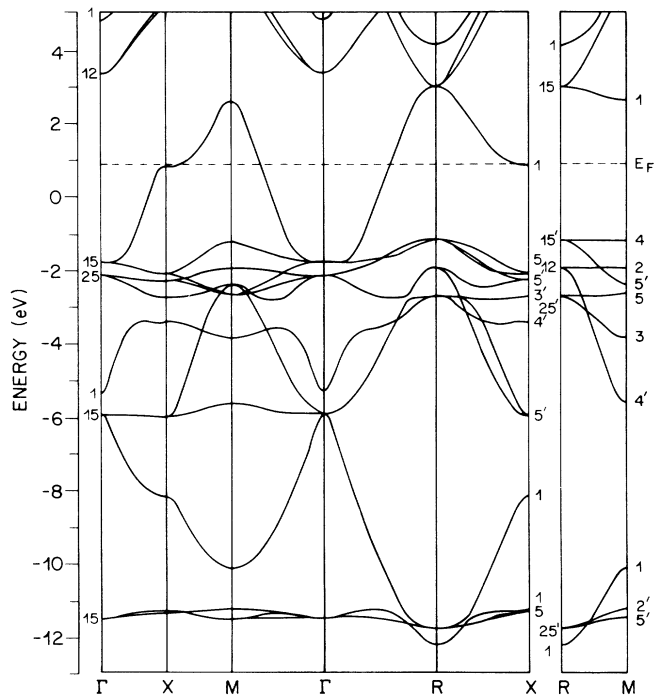


FIG. 1. LAPW energy-band results for simple-cubic BaBiO₃. The energy zero reflects the band filling (i.e., minus one-half an electron) for the 50-50 alloy, Ba_{0.5}K_{0.5}BiO₃.

mations on either the charge density or the potential. Exchange and correlation effects are treated with the use of the Wigner interpolation formula.¹⁵ The atomic Ba($5p^6 6s^2$), K($3p^6 4s$), Bi($6s^2 6p^3$), and O($2s^2 2p^4$) states are included as valence bands, while the more tightly-bound corelike states are handled with a frozen-core approximation.¹⁴

The simplest three ordered 50-50 Ba_{0.5}K_{0.5}BiO₃ alloys contain two formula units per primitive cell and involve alternating planes of Ba and K atoms along [001], [110], and [111] directions, respectively. The first case leads to a doubling of the unit cell along the c axis, while the second involves basal-plane ordering with a 45° rotated $\sqrt{2} \times \sqrt{2}$ superlattice. The [111] alternation places the Ba and K atoms on a rocksalt-type lattice. The resulting phases can be described¹¹ as chemical ordering waves with wave vectors \mathbf{q} equal to those at the X , M , and R points on the surface of the simple-cubic Brillouin zone.⁷ They have either tetragonal (X, M) or cubic (R) symmetry and the appropriate space groups are $P4/mmm$ and $Fm\bar{3}m$, respectively.

Because of the additional complexity that is introduced by the doubling of the unit-cell size for the BaKBi₂O₆ ordered alloys, it is useful to utilize the simple-cubic band structure of BaBiO₃ as a reference. Accordingly, LAPW calculations have been carried out for this phase with the observed³ lattice parameter

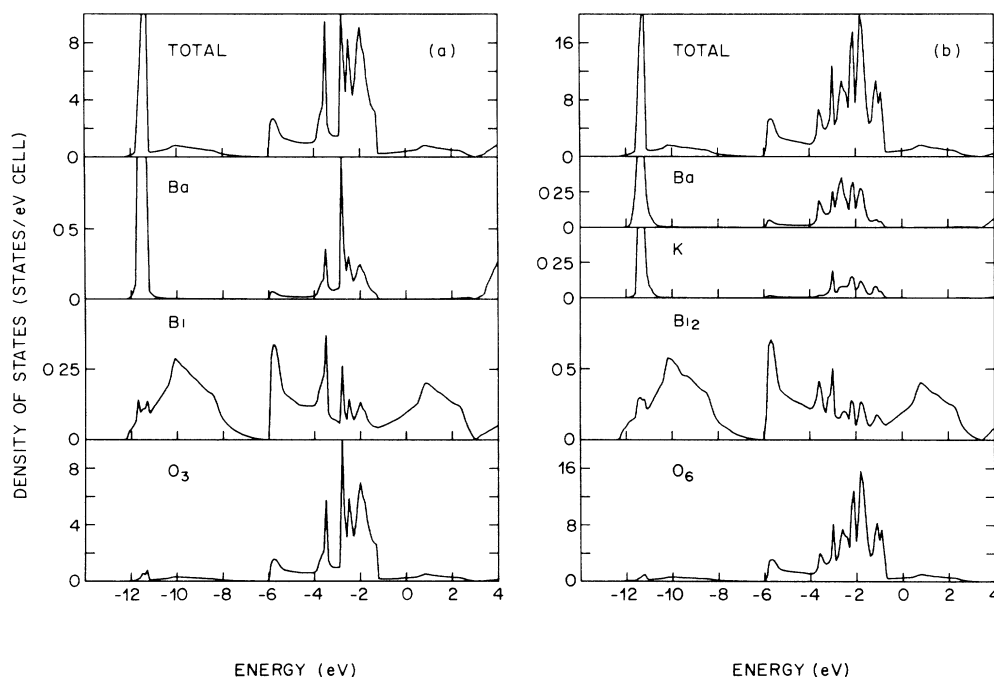


FIG. 2. Total and muffin-tin-projected density-of-states results for (a) cubic BaBiO₃, and (b) the tetragonal ordered BaKBi₂O₆ alloy with alternating K and Ba planes along c . The energy zero in (a) corresponds to the band filling in (b). The units in each sub-panel are scaled to facilitate direct comparison of the results.

($a = 4.29 \text{ \AA}$) for $\text{Ba}_{0.6}\text{K}_{0.4}\text{BiO}_3$. The results, which are shown in Fig. 1, are in close agreement with those obtained previously (Fig. 5 of Ref. 7) with the slightly larger ($\approx 1.4\%$) averaged cubic lattice parameter of pure BaBiO_3 . The Fermi level cuts through the uppermost band of a ten-band $\text{Bi}(6s)\text{-O}(2p)$ complex. The flat low-lying bands correspond to Ba $5p$ states while the uppermost complex of unoccupied bands is derived from Ba $5d$ and Bi $6p$ states.

The $\text{Bi}(6s)\text{-O}(2p)$ manifold features a pair of broad ($\approx 16 \text{ eV}$) σ -bonding and antibonding subbands that extend (at R) from -12 to $+4 \text{ eV}$, the latter being half filled. The narrower intermediate bands are derived from weaker-bonding $\text{O}(2p)$ orbitals, including those oriented perpendicular to the nearest-neighbor Bi-O bond directions. The essential features of these $\text{Bi}(6s)\text{-O}(2p)$ bands can be summarized in terms of simple tight-binding models.⁵⁻⁹

The overall effect of K alloying is illustrated by the density-of-states (DOS) results in Fig. 2. Here, we compare the DOS results for our reference compound, cubic BaBiO_3 , with that calculated for the tetragonal BaKBi_2O_6 ordered alloy with alternating (001) planes of Ba and K, which we describe as a $\mathbf{q}=\mathbf{X}$ ordering wave. Except for modifications to the "spiky" structure in the energy range of -2 to -4 eV , the total and muffin-tin-projected DOS results for both compounds are in excellent agreement. It is interesting to note that the $\text{K}(3p)$ and $\text{Ba}(6p)$ corelike states are nearly degenerate. A noticeable difference between the results is the presence of a DOS peak at $\approx -1 \text{ eV}$ in Fig. 2(b) that extends to the high DOS region $\approx 0.5 \text{ eV}$ above that in Fig. 2(a). This is due primarily to $\text{O}(2p)$ states which are localized in the K layers. These are shifted upwards relative to the other O states by Madelung effects, reflecting the smaller ionic charge of K. It is expected that such effects will be reduced for the other 50-50 alloys since each O then has pairs of nearest-neighbor Ba and K ions rather than a unique O site with only K neighbors.

A detailed comparison between the x -dependent DOS

TABLE I. Calculated dependence of the density of states on x in $\text{Ba}_{1-x}\text{K}_x\text{BiO}_3$ -type alloys, with the assumption of a rigid-band variation with band filling for the present BaBiO_3 and $\text{Ba}_{0.5}\text{K}_{0.5}\text{BiO}_3$ ($\mathbf{q}=\mathbf{X}$) results.

x	BaBiO_3 (states/eV)	$\text{Ba}_{0.5}\text{K}_{0.5}\text{BiO}_3$ (states/eV)
0.75	0.26	0.33
0.6	0.33	0.38
0.5	0.39	0.42
0.4	0.44	0.46
0.2	0.64	0.67
0.0	0.80	0.80

results near E_F for the reference compound BaBiO_3 and the $\mathbf{q}=\mathbf{X}$ ordered alloy BaKBi_2O_6 is contained in Table I. These results agree to within $\approx (5-10)\%$ for $0.0 < x < 0.5$, though the deviations increase for higher x . Note that the present $x=0.75$ rigid-band value that is derived from the BaBiO_3 results is in excellent agreement with the corresponding $y=0.25$ value⁸ (0.26 vs 0.24 state/eV cell) for $\text{BaPb}_{1-y}\text{Bi}_y\text{O}_3$ when the x, y values are fixed ($x=1-y$) to produce the same band filling. These results suggest that a similar rigid-band picture should also hold for A -site-doped $\text{Ba}_{1-x}\text{T}_x\text{PbO}_3$, where a trivalent dopant T would raise E_F toward half filling.

A direct measure of superlattice effects near E_F is provided by plots of the LAPW conduction bands in the appropriate Brillouin-zone faces for the three ordered BaKBi_2O_6 alloys which are considered here. These results are plotted in Figs. 3(a), 3(b), and 3(c) for the $\mathbf{q}=\mathbf{X}$, \mathbf{M} , and \mathbf{R} superlattices, respectively. In each case, these splittings are extremely small near E_F , less than the size (0.1 eV) of the squares that represent the results. Larger splittings ($\approx 0.2-0.5 \text{ eV}$) occur near the band extrema. It is emphasized that the maximum su-

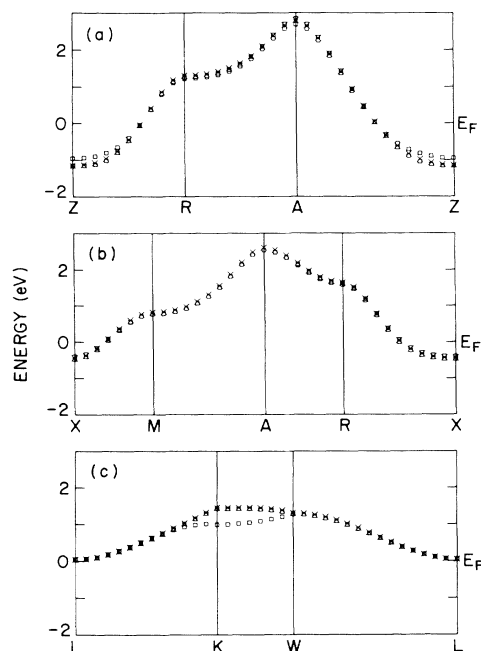


FIG. 3. Superlattice splittings near E_F for the LAPW conduction bands of three ordered BaKBi_2O_6 alloys (square symbols). Individual results are plotted along symmetry lines in the appropriate folding-induced Brillouin-zone faces for K ordering waves with (a) $\mathbf{q}=\mathbf{X}$, (b) $\mathbf{q}=\mathbf{M}$, and (c) $\mathbf{q}=\mathbf{R}$, respectively. The crosses denote the corresponding (doubly degenerate) results for the reference material, cubic BaBiO_3 (Fig. 1). The abscissa is labeled by the symmetry points of the appropriate tetragonal [(a) and (b)] and fcc [(c)] Brillouin zones with standard notation.

perlattice effects are expected for wave vectors in these "folding planes," where the reference results (denoted by the crosses) are degenerate. Perturbation-theory arguments suggest that deviations are further suppressed by energy denominators at other wave vectors. On the basis of these results, it seems unlikely that Weber's mechanism¹¹ could produce a nonmetallic phase in $\text{Ba}_{1-x}\text{K}_x\text{BiO}_3$ or the proposed $\text{Ba}_{1-x}\text{T}_x\text{PbO}_3$ alloys.

In summary, we have shown that superlattice effects caused by substitutional K doping on the A site in $\text{Ba}_{1-x}\text{K}_x\text{BiO}_3$ have a minimal effect on the electronic states near E_F , confirming the inactive nature of this site. This suppresses Weber's mechanism¹¹ and extends the metallic regime of these alloys closer to half filling, where the deformation potentials for breathing-type O displacements (Fig. 13 of Ref. 7) and the electron-phonon interaction¹³ are at maxima. Indeed, in contrast to the cuprates, a CDW-induced distortion is observed¹⁰ for the parent semiconductor, BaBiO_3 . This suggests that the observed superconducting properties can be explained in terms of the conventional phonon mechanism. A magnetic mechanism would be surprising in this class of materials because of the itinerant nature of the Bi 6s conduction electrons. Finally, it is noted that even higher T_c 's may be possible if a near-cubic perovskite phase of $\text{Ba}_{1-x}\text{K}_x\text{BiO}_3$ or $\text{Ba}_{1-x}\text{T}_x\text{PbO}_3$ can be stabilized closer to half filling without producing inhomogene-

ous multiphase samples.

¹J. G. Bednorz and K. A. Müller, Z. Phys. B **64**, 189 (1986); J. G. Bednorz, M. Takashigi, and K. A. Müller, Europhys. Lett. **3**, 379 (1987).

²L. F. Mattheiss, E. M. Gyorgy, and D. W. Johnson, Jr., Phys. Rev. B **37**, 3745 (1988).

³R. J. Cava *et al.*, Nature (London) **332**, 814 (1988).

⁴A. W. Sleight, J. L. Gillson, and P. E. Bierstedt, Solid State Commun. **17**, 27 (1975).

⁵L. F. Mattheiss and D. R. Hamann, Phys. Rev. B **26**, 2686 (1982).

⁶L. F. Mattheiss and D. R. Hamann, in *Superconductivity in d- and f-band Metals*, edited by W. Buckel and W. Weber (Kernforschungszentrum Karlsruhe, Karlsruhe, Federal Republic of Germany, 1982), p. 405.

⁷L. F. Mattheiss and D. R. Hamann, Phys. Rev. B **28**, 4227 (1983).

⁸L. F. Mattheiss, Phys. Rev. B **28**, 6629 (1983).

⁹L. F. Mattheiss, Jpn. J. Appl. Phys. **24**, Suppl. 2,6 (1985).

¹⁰D. E. Cox and A. W. Sleight, Solid State Commun. **19**, 969 (1976), and Acta Crystallogr. Sect. B **35**, 1 (1979).

¹¹W. Weber, Jpn. J. Appl. Phys. **26**, Suppl. 3, 981 (1987).

¹²K. Takegahara and T. Kasuya, J. Phys. Soc. Jpn. **56**, 1478 (1987).

¹³W. Weber and L. F. Mattheiss, unpublished.

¹⁴L. F. Mattheiss and D. R. Hamann, Phys. Rev. B **33**, 823 (1986).

¹⁵E. Wigner, Phys. Rev. **46**, 1002 (1934).